



Published in final edited form as:

*BJOG*. 2016 June ; 123(7): 1076–1085. doi:10.1111/1471-0528.13514.

## The impact of prolapse mesh on vaginal smooth muscle structure and function

Z Jallah<sup>a</sup>, R Liang<sup>b</sup>, A Feola<sup>c</sup>, W Barone<sup>a</sup>, S Palcsey<sup>b</sup>, SD Abramowitch<sup>a,b</sup>, N Yoshimura<sup>d</sup>, and P Moalli<sup>a,b</sup>

<sup>a</sup>Musculoskeletal Research Center, Department of Bioengineering, University of Pittsburgh, Pittsburgh, PA, USA

<sup>b</sup>Magee-Womens Research Institute, Department of Obstetrics, Gynecology and Reproductive Science, University of Pittsburgh, Pittsburgh, PA, USA

<sup>c</sup>Department of Biomedical Engineering, Georgia Institute of Technology, Atlanta, Georgia, USA

<sup>d</sup>Department of Urology, University of Pittsburgh School of Medicine, Pittsburgh, PA, USA

### Abstract

**Objective**—To evaluate the impact of prolapse meshes on vaginal smooth muscle structure (VaSM) and function, and to evaluate these outcomes in the context of the mechanical and textile properties of the mesh.

**Design**—Three months following the implantation of three polypropylene prolapse meshes with distinct textile and mechanical properties, mesh tissue explants were evaluated for smooth muscle contraction, innervation, receptor function, and innervation density.

**Setting**—Magee-Womens Research Institute at the University of Pittsburgh.

**Population**—Thirty-four parous rhesus macaques of similar age, parity, and pelvic organ prolapse quantification (POP-Q) scores.

**Methods**—Macaques were implanted with mesh via sacrocolpopexy. The impact of Gynemesh™ PS (Ethicon;  $n = 7$ ), Restorelle® (Coloplast;  $n = 7$ ), UltraPro™ parallel and UltraPro™ perpendicular (Ethicon;  $n = 6$  and  $7$ , respectively) were compared with sham-operated controls ( $n$

---

*Correspondence:* Dr P Moalli, Associate Professor, Magee-Womens Research Institute, 204 Craft Avenue, Pittsburgh, PA 15213, USA. pmoalli@mail.magee.edu.

#### Disclosure of interests

None declared. Completed disclosure of interests form available to view online as supporting information.

#### Contribution to authorship

ZJ – planning and performing of experiments for histological and biochemical end points, analysing data, and drafting of the article; RL – surgery, carrying out of experiments for histological end points, and drafting of the article; AF – planning and surgery; WB – planning and surgery; SP – surgery and carrying out experiments for histological end points; SA – study conception, planning, surgery, and drafting of article; NY – study conception, planning, and drafting of article; PM – study conception, surgery, planning, analyzing data, and drafting of article.

#### Details of ethics approval

This study was conducted with the approval of the University of Pittsburgh's Institutional Animal Care Use Committee (IACUC #1008675), and in adherence with the National Institutes of Health Guidelines (approval date 6 August 2010).

#### Supporting Information

Additional Supporting Information may be found in the online version of this article:

= 7). Outcomes were analysed by Kruskal–Wallis ANOVA, Mann–Whitney *U*-tests and multiple regression analysis ( $P < 0.05$ ).

**Mean outcome measures**—Vaginal tissue explants were evaluated for the maximum contractile force generated following muscle, nerve, and receptor stimulation, and for peripheral nerve density.

**Results**—Muscle myofibre, nerve, and receptor-mediated contractions were negatively affected by mesh only in the grafted region ( $P < 0.001$ ,  $P = 0.002$ , and  $P = 0.008$ , respectively), whereas cholinergic and adrenergic nerve densities were affected in the grafted ( $P = 0.090$  and  $P = 0.008$ , respectively) and non-grafted ( $P = 0.009$  and  $P = 0.005$ , respectively) regions. The impact varied by mesh property, as mesh stiffness was a significant predictor of the negative affect on muscle function and nerve density ( $P < 0.001$  and  $P = 0.013$ , respectively), whereas mesh and weight was a predictor of receptor function ( $P < 0.001$ ).

**Conclusions**—Mesh has an overall negative impact on VaSM, and the effects are a function of mesh properties, most notably, mesh stiffness.

### Keywords

Peripheral nerves; polypropylene mesh; smooth muscle

### Introduction

Pelvic organ prolapse (POP) is a condition characterised by a loss of support to the vagina, resulting in the descent of the pelvic organs. POP affects over one-half of women over 50 years of age, and advanced stages are associated with a decrease in quality of life.<sup>1</sup> In the USA, the lifetime risk of undergoing surgical repair for symptomatic POP is 7%, with direct annual costs estimated to exceed \$1 billion.<sup>2,3</sup> Surgical repair can involve the placement of a permanent synthetic polypropylene mesh to restore the prolapsed organs to their anatomical position; however, 10% of patients who receive mesh have complications, despite the introduction of lightweight ( $<45 \text{ g/m}^2$ ), large-pore ( $>1 \text{ mm}^2$ ), monofilament polypropylene meshes to the market.<sup>4,5</sup> The prevalence of these complications, including exposure, erosion, pain, and infection, resulting especially from transvaginal repairs, have prompted warnings from the US Food and Drug Administration. The most recent public health notification appeared in 2011, warranting more thorough investigations into mechanisms by which mesh may negatively affect the vagina.<sup>6</sup>

Previously, we showed that implantation of mesh by sacrocolpopexy increases apoptosis and decreases the thickness of vaginal smooth muscle (VaSM) in the underlying and newly incorporated vagina.<sup>7,8</sup> Interestingly, the degree of impact varied with each mesh, but these meshes are typically marketed similarly, and are used interchangeably in clinical settings. When paired with a previous study of ours, which showed variability in the textile and mechanical properties of meshes, these findings suggest that minor differences in mesh properties could be contributing to differing outcomes.<sup>9</sup> For example, the widely used Gynemesh™ PS (Ethicon) was associated with the greatest negative impact on smooth muscle relative to two lower stiffness meshes, UltraPro™ (Ethicon) and Restorelle® (Coloplast).<sup>9</sup> As VaSM plays an essential role in maintaining vaginal function (e.g. tone),

and is compromised in women with prolapse, it is essential that its structure and function, at the very least, be preserved if not improved following surgery.<sup>10–14</sup>

The results from the previously cited studies suggest that lower stiffness and lighter weight meshes be used to achieve the aforementioned goal, but the mechanism(s) remains unclear. Hence, to further investigate the mechanism of impact, this study evaluated the effect of mesh implantation on VaSM myofibre, innervation, receptor function, and innervation density, in the underlying grafted tissues and tissues adjacent to the mesh (non-grafted tissues).

## Methods

### Animals

All non-human primates (NHP) (*Macacca mulatta*, rhesus macaques) used in this study were maintained and treated according to an experimental protocol approved by the Institutional Animal Care and Use Committee of the University of Pittsburgh (IACUC #1008675), and were in adherence with the National Institutes of Health guidelines. Animals were maintained in standard cages with water (*ad libitum*) and scheduled monkey diet, supplemented with fresh fruits, vegetables, and multiple vitamins, daily. A 12-hour light/dark cycle (07:00–19:00 h) was used, and menstrual cycle patterns were recorded daily. Available demographic data of each NHP were collected prior to and after surgery, including age, weight, gravidity, and parity. Researchers were blinded to all demographic data of each primate until completion of the study.

### Surgical procedures

Thirty-four cycling parous rhesus macaques without prolapse were selected for sham ( $n = 7$ ) or mesh implantation. For the study the high stiffness mesh, Gynemesh™ PS (Ethicon;  $27.5 \pm 2.7$  N/mm), was implanted, as well as two lower stiffness meshes, UltraPro™ (Ethicon;  $0.01 \pm 0.00$  N/mm) and Restorelle® (Coloplast;  $0.18 \pm 0.03$  N/mm). Additionally, UltraPro™, which is highly anisotropic, was implanted with its blue orientation lines perpendicular to the long axis of the vagina, as is performed clinically (UltraPro™ perpendicular – low stiffness direction,  $0.01 \pm 0.00$  N/mm;  $n = 6$ ), and also with its blue orientation lines parallel with the long axis of the vagina (UltraPro™ parallel – high stiffness direction,  $0.26 \pm 0.09$  N/mm,  $n = 7$ ), so as to evaluate the influence of stiffness independently of changes in mesh weight and porosity. Following completion of the hysterectomy, and vaginal and presacral dissections, each primate was randomised on the day of surgery to a mesh group or to the sham control group. All meshes were implanted by abdominal sacrocolpopexy following hysterectomy, as previously published.<sup>7,8</sup> This design ensured that the impact of mesh was being evaluated, independent of the degenerative effects of the POP (which could be variable), and following a procedure that has been shown with level-I clinical evidence to be associated with minimal complications. Twelve weeks after surgery, the vagina was dissected *in toto*, and immediately following acquisition, biopsies were obtained from a region of the anterior vagina underlying the mesh (grafted) and from a region adjacent to the mesh (non-grafted).

### Functional assay: tissue organ bath

For the organ bath assay, grafted and non-grafted tissues were subsequently divided into four 2 mm × 7 mm circumferential strips. In order to perform accurate comparisons, biopsies analysed from the sham group were taken from regions corresponding to where the mesh was placed in the mesh-implanted animals, and adjacent to it, and labelled as sham grafted and non-grafted, respectively. The tissues were tested as previously described.<sup>15</sup> Analysis of muscle myofibre function was measured by the force generated following muscle depolarisation by a high-concentration potassium solution (KCl: 120 mM), innervation function was measured by the force generated following electrical field stimulation (EFS: 1 Hz), and receptor function was measured by the force generated following receptor depolarisation by a non-selective muscarinic and  $\alpha_1$ -adreno-receptor agonist (carbachol and phenylephrine: from  $10^{-8}$  to  $10^{-4}$  M, non-cumulatively). After the observed response had plateaued following the application of each dose, the tissues were washed with Krebs solution three times (10 minutes for each wash), and the next dose was applied. The contractile force generated in response to EFS, carbachol, and phenylephrine was normalised to the force generated following KCl application. With 120 mM KCl proven to fully depolarise the smooth muscles, partial nerve depolarisation or receptor activation would only yield a percentage of the contractile force generated by KCl, thus providing an opportunity to capture functional changes. Additionally, to ensure that the changes observed were not a result of changes in muscle myofibre function, normalisation to the KCl response was necessary.

### Histochemical and immunohistochemical assay: muscle and nerves

For the histochemical and immunohistochemical assays, grafted and non-grafted tissues were fixed in 4% paraformaldehyde, embedded in Optimal Cooling Temperature (OCT) compound, and cryosectioned at 10- $\mu$ m thickness, followed by Masson's trichrome staining, according to the methods of the Center for Biological Imaging (CBI, University of Pittsburgh). Protein gene product (PGP 9.5), a neuron-specific ubiquitin that localises to neuronal axons, was used to evaluate peripheral nerve density (1:10 000; rabbit polyclonal antibody, YBG78630507; Accurate Chemical, Westbury, NY, USA). Vesicular acetylcholine transporter (VAcHT), which is localised within the soma and the axons of cholinergic neurons, plays a role in the packaging and transporting of acetylcholine (ACh) into synaptic vesicles (1:5000 rabbit monoclonal antibody; V5387; Sigma-Aldrich, St. Louis, MO, USA). Lastly, tyrosine hydroxylase (TH), a rate-limiting enzyme that converts L-tyrosine to L-DOPA, which is then converted to dopamine (a precursor of norepinephrine), was used to identify adrenergic nerve fibres (1:1000; rabbit polyclonal antibody, T8700; Sigma-Aldrich). Following incubation with the primary antibodies, the sections were incubated for 4 hours at 4°C with Cy3 or FITC-conjugated f(ab) donkey anti-rabbit IgG (1:100; no. 711 165 152; Jackson Laboratories, Bar Harbor, ME, USA), diluted in PBDT [phosphate buffered saline (PBS), 0.3% triton, and 2% donkey serum (Jackson Laboratories, #017-000-001)]. In control experiments, no immunofluorescence staining was observed when the primary antiserum was omitted.

## Morphometric analysis

All images were captured using a Nikon microscope, synced with a Nikon colour digital camera, before being imported into ELEMENTS 3.2 (NIS-Elements AR) for quantification. To evaluate fibres immunoreactive (IR) for PGP 9.5, VAcHt, and TH in the three regions of the vagina, images were randomly captured at 10× magnification. For analysis, all images were acquired, and the same threshold was applied. Pixels of binary images in which the intensity did not exceed the threshold value were automatically removed and considered negative. The numbers of profiles per unit area of the vaginal wall for the vaginal layers was measured (% fractional area) and averaged for each section.

## Statistical methods

Statistical analysis of functional (maximum force), and histological (% fractional area) outcomes of VaSM myofibre, nerve, and receptor function were performed using IBM SPSS 17.0 (SPSS Inc., Armonk, NY, USA). Differences between mesh groups were evaluated using Kruskal–Wallis tests, and Bonferonni post-hoc tests. For additional analysis of UltraPro™ Perpendicular versus UltraPro™ Parallel, and grafted versus non-grafted regions, Mann–Whitney *U*-tests were used. Regression and correlation analysis were then performed to evaluate the influence of mesh properties on these outcomes. For all measures, significance was set at  $P < 0.05$ , and all *P* values presented have been corrected. These analyses were performed to aid in determining whether the negative impact of mesh on VaSM is the result of a loss of muscle contractile elements, a loss of innervation, or a loss of receptor function, and if these changes are a function of mesh textile and mechanical properties. Additionally, the evaluation of both grafted and non-grafted tissues will provide verification of the extent of the impact on the vagina.

## Results

There were no significant differences in the age, weight, and parity of the NHP groups (Table 1) prior to implantation with the three meshes of variable textile properties (Table S1);<sup>8</sup> however, upon explantation, the grafted region, shown as the boxed area in Figure 1, was distinct from the non-grafted region, and this grafted region was visually variable between groups. The mesh in the grafted region had evidence of host tissue ingrowth (Figure 1A–D), with the degree of incorporation varying according to the stiffness of the mesh implanted (Figure 1E–H). Specifically, at the mesh–tissue interface, UltraPro™ perpendicular and Restorelle® had better tissue incorporation, whereas Gynemesh™ PS and UltraPro™ parallel appeared buckled, and surrounded by a capsule of connective tissue (Figure 1A–D). Immunohistochemical and functional characteristics following mesh implantation are summarised in Tables 2 and 3, but detailed interpretations of the results are as follows.

## Muscle-mediated contractions

In the grafted region, evaluation of the contractile force generated following KCl administration showed that muscle myofibre function significantly differed between the groups ( $P < 0.001$ ) (Table 2). The grafted region of Gynemesh™ PS, UltraPro™ parallel (high stiffness), and Restorelle® generated significantly less force relative to sham ( $P <$

0.001,  $P < 0.001$ , and  $P = 0.015$ , respectively), but UltraPro™ perpendicular did not ( $P = 0.155$ ). As shown in Table 2, the decrease in contractile force following implantation of Gynemesh™ PS and UltraPro™ parallel was the greatest at 80 and 65%, respectively. Comparison of the contractile force generated by UltraPro™ parallel and UltraPro™ perpendicular showed a trend towards less force generation by the stiffer UltraPro™ parallel ( $P = 0.078$ ). In the non-grafted region, the difference was not significant but there was a trend toward differences between the groups ( $P = 0.085$ ), and UltraPro™ parallel again showed a trend towards less force generation than UltraPro™ perpendicular ( $P = 0.052$ ).

### Nerve-mediated contractions

In the grafted region, the contractile force generated following EFS showed that nerve function was significantly different between the groups ( $P = 0.002$ ; Table 2). Nerve-mediated contractile force generated following implantation with Gynemesh™ PS significantly decreased by 91% relative to sham-operated controls ( $P = 0.008$ ); however, there was no significant decrease following implantation with the lower stiffness UltraPro™ perpendicular and Restorelle® ( $P = 0.187$  and  $P = 0.155$ , respectively). Comparison of the contractile force generated by UltraPro™ parallel and Ultra-Pro™ perpendicular showed no significant difference ( $P = 0.143$ ). In the non-grafted region, there was also no significant difference in nerve function between the groups ( $P = 0.361$ ), and UltraPro™ parallel and UltraPro™ perpendicular were similar ( $P = 0.247$ ).

### Receptor-mediated contractions

In the grafted region, contractile force generated following the application of the muscarinic agonist, carbachol, showed that muscarinic receptor function was significantly different between the groups ( $P = 0.008$ ; Table 2). Of note, there was a 90% decline in the receptor-mediated contractile force generated following implantation with Gynemesh™ PS ( $P = 0.007$ ), whereas there was a 62% increase in the contractile force generated following implantation with Restorelle® ( $P = 0.037$ ). Comparison of the contractile force generated by UltraPro™ parallel and UltraPro™ perpendicular showed no significant difference ( $P = 0.999$ ). In the non-grafted region, there was no significant difference in cholinergic receptor function between the groups ( $P = 0.148$ ), and UltraPro™ parallel was not significantly different from UltraPro™ perpendicular ( $P = 0.647$ ).

The contractile force generated following application of the adrenergic receptor agonist phenylephrine (from  $10^{-8}$  to  $10^{-4}$  M, non-cumulatively) was not substantial and was rendered unquantifiable, whereas a robust response in our positive control (primate bladder) was observed. This could be because of a downregulation of the  $\alpha_1$ -adrenoreceptors, as has been shown to occur with childbirth or surgery.<sup>19</sup>

### Histochemical and immunohistochemical assays

**Muscle morphology**—Masson's trichrome staining of the grafted region showed dense and organised smooth muscle bundles in the sham-operated animals, relative to all mesh-implanted animals (Figure 2). Following Gynemesh™ PS implantation there was increased disruption and decreased size of the muscle bundles in the grafted region, as well as a decrease in the thickness of the muscle layer (Figure 2B). UltraPro™ parallel also appeared



to have an effect on the size of the muscle bundles, but the thickness of the muscle layer was preserved, as there was less migration of the mesh into the smooth muscle layer compared with Gynemesh™ PS. In contrast, UltraPro™ perpendicular and Restorelle® were observed to have minimal negative effect on the smooth muscle bundles, organization, and thickness in the grafted region (Figure 2E). In the non-grafted region, these changes were less visible, supporting the trends in the functional data.

**Peripheral nerve density**—In the grafted region, peripheral nerve density was significantly different between the groups ( $P < 0.001$ ; Table 3). There were fewer peripheral nerves present following Gynemesh™ PS and UltraPro™ parallel implantation, relative to sham ( $P < 0.001$  and  $P < 0.001$ , respectively), but Restorelle® and UltraPro® perpendicular were not significantly different ( $P = 0.159$  and  $P = 0.110$ ; Figure 3A–D). Comparison of peripheral nerve density between UltraPro™ parallel and UltraPro™ perpendicular showed a trend towards reduced nerve density in the stiffer UltraPro™ parallel ( $P = 0.088$ ). In the non-grafted region, there was no significant difference in nerve density between the groups ( $P = 0.157$ ), and UltraPro™ parallel was not significantly different from UltraPro™ perpendicular ( $P = 0.684$ ).

**Cholinergic nerve density**—In the grafted region, cholinergic nerve density did not significantly differ between the groups ( $P = 0.093$ ; Table 3). Comparison of nerve density following implantation with UltraPro™ parallel and UltraPro™ perpendicular also showed no significant difference ( $P = 0.146$ ). Interestingly, in the non-grafted region, there was a significant difference between the groups ( $P = 0.009$ ), with a trend toward less cholinergic nerve density following implantation with Gynemesh™ PS, supporting the loss in nerve function ( $P = 0.077$ ). In contrast, there was a trend towards increased cholinergic nerve density following implantation of the less stiff UltraPro™ perpendicular and Restorelle® ( $P = 0.055$  and  $P = 0.099$ , respectively; Figure S1). Comparison of cholinergic nerve density in UltraPro™ parallel and UltraPro™ perpendicular also showed a significant difference ( $P = 0.028$ ), which may explain the trend towards an increase in nerve density with the less stiff meshes.

**Adrenergic nerve density**—In the grafted region, adrenergic nerve density was significantly different between the groups ( $P = 0.008$ ; Table 3). There were less adrenergic nerves present following Gynemesh™ PS and UltraPro™ parallel implantation, relative to sham ( $P = 0.004$ ,  $P = 0.013$ ), but less stiff Restorelle® and UltraPro® perpendicular were not significantly different ( $P = 0.848$  and  $P = 0.121$ , respectively). Comparison of adrenergic nerve density in UltraPro™ parallel and Ultra Pro™ perpendicular, showed no significant difference ( $P = 0.464$ ). In the non-grafted region, there was also a significant difference in adrenergic nerve density between the groups ( $P = 0.005$ ). Similar to the grafted region, nerve density decreased following Gynemesh™ PS implantation and UltraPro™ parallel implantation ( $P = 0.004$ ,  $P = 0.011$ , respectively), but was not significantly different following implantation with Restorelle® or UltraPro™ perpendicular ( $P = 0.848$ ,  $P = 0.121$ , respectively) (Figure S1, row 2). Comparison of adrenergic nerve density in UltraPro™ parallel to UltraPro™ perpendicular also showed no significant difference ( $P = 0.223$ ).

## Relationship between mesh properties and smooth muscle outcomes

Correlational analysis showed a relationship between the smooth muscle functional outcome measures (contraction, innervation, and receptor function) and mesh properties, and these trends were similar for the histological analysis (not shown). Specifically, mesh stiffness was negatively correlated with outcome measures in both the grafted [Spearman  $\rho = -0.567$  ( $P = 0.001$ ),  $\rho = 0.718$  ( $P < 0.001$ ), and  $\rho = -0.444$  ( $P = 0.018$ )] and non-grafted [Spearman  $\rho = -0.398$  ( $P = 0.029$ ),  $\rho = -0.398$  ( $P = 0.029$ ),  $\rho = -0.398$  ( $P = 0.029$ )] regions. Similar to mesh stiffness, mesh weight was also negatively correlated with the outcome measures, but only in the grafted region [Spearman  $\rho = -0.427$  ( $P = 0.019$ ),  $\rho = -0.711$  ( $P < 0.001$ ), and  $\rho = -0.605$  ( $P = 0.001$ )], whereas mesh porosity was positively correlated with smooth muscle outcomes in the grafted region [Spearman  $\rho = 0.427$  ( $P = 0.019$ ),  $\rho = 0.711$  ( $P < 0.001$ ), and  $\rho = 0.606$  ( $P < 0.001$ )].

In addition to confirmation of a relationship between the outcome measures and mesh properties, regression analysis further showed that the outcomes measures could be predicted by the mesh properties (Table 4). Specifically, mesh stiffness was shown to be the single significant influencer of muscle contraction in both the grafted and non-grafted regions ( $P < 0.001$  and  $P = 0.001$ , respectively). Mesh stiffness was also shown to influence peripheral nerve density in both the grafted and non-grafted regions ( $P = 0.013$ ,  $P = 0.049$ , respectively), but so was mesh weight ( $P = 0.007$  and  $P < 0.001$ , respectively). Unlike mesh stiffness, however, mesh weight also had an influence on receptor function in the grafted region ( $P < 0.001$  and  $P = 0.002$ , respectively). An evaluation of mesh porosity again showed an influence on peripheral nerve density ( $P = 0.033$ ), and similar to mesh weight, porosity also had a significant influence on receptor function ( $P = 0.002$ ).

## Discussion

### Main findings

Prolapse meshes Restorelle® (Coloplast), UltraPro™ (Ethicon), and Gynemesh™ PS (Ethicon), which are used interchangeably in clinical settings, with seemingly minor differences in textile and mechanical properties, resulted in variable outcomes following implantation. It was immediately apparent upon excision of the mesh-implanted vaginas that the less stiff UltraPro™ perpendicular and Restorelle® were better incorporated into the tissue than the stiffer Gynemesh™ PS, which appeared buckled and surrounded by a capsule of connective tissue. Implantation of the stiffer Gynemesh™ PS was also associated with the greatest loss in muscle thickness, which was accompanied by a decrease in muscle myofibre function, nerve function, and receptor function in the grafted region. In general, UltraPro™ parallel, which has comparable stiffness to that of Gynemesh™ PS, had a similar degree of impact, whereas the less stiff Restorelle® had less of an impact, and the least stiff mesh, UltraPro™ perpendicular, had minimal impact. The observed responses mirrored the stiffness profiles of the meshes, and upon statistical evaluation, mesh stiffness proved to be a significant predictor of smooth muscle function in both the grafted and non-grafted regions, whereas the observed changes in nerve- and receptor-mediated contractions were shown to be a function of not only mesh stiffness but also of mesh weight and porosity.



Further quantification of peripheral nerve density in the grafted region also showed a significant decline following implantation with Gynemesh™ PS and UltraPro™ parallel, but not following implantation with UltraPro™ perpendicular and Restorelle®. Gynemesh™ PS significantly decreased cholinergic nerve density in the non-grafted region, whereas implantation with UltraPro™ perpendicular and Restorelle® caused an increase in cholinergic nerve density, albeit non-significantly. Subsequent analysis of adrenergic nerves showed that implantation with Gynemesh™ PS and UltraPro™ parallel significantly decreased adrenergic nerve density in both the grafted and non-grafted regions. The finding of variable effects of mesh from what would appear to be negligible differences in textile and mechanical properties of clinically used prolapse meshes is enlightening.

### Strengths and limitations

Although relevant and timely, this work is not without limitations. The use of non-human primates without proplase in this study is indeed limiting, but nevertheless allows for ease of application when designing future clinical studies to further evaluate sources of complications in women with prolapse due to the similarity in pelvic floor anatomy. As is, our analysis also had sufficient statistical power to show significant differences between each mesh, as well as the influence of specific mesh properties. However, as a result of the design of the study, we are also unable to definitively state whether the loss of innervation and receptor function precedes the decline in VaSM myofibre function and thickness, although abundant literature is in support of this mechanism. Finally, as all evaluations were conducted at 3 months post-implantation, it is likely that the effect of mesh stiffness may be more pronounced at a later time point, and that the effects of subtle changes in mesh properties may become negligible, as these changes may simply be altering the time course of remodelling.

### Interpretation

The use of synthetic polypropylene mesh for prolapse surgery was originally adopted by clinicians because of the long-term anatomical support that it provides, and as clinical successes soared, the widespread use of mesh ensued as well as the advent of multiple mesh products on the market.<sup>16–18</sup> The increased use of mesh has been paralleled by rising complication rates, however, which has prompted the need for studies aimed at elucidating possible sources of complications.<sup>4,5</sup> To this end, the detailed histological and functional data from this study on the variable negative impacts of clinically used synthetic meshes on VaSM myofibre, nerve, and receptor function is highly relevant.

The surprising finding of the increased encapsulation of Gynemesh™ PS is supported by recent studies, which show that stiffer implants promote increased macrophage phagocytosis, migration, proliferation, differentiation, adhesion, and expression of the pro-inflammatory cytokine TNF- $\alpha$ .<sup>20–24</sup> This would suggest that, Gynemesh™ PS, the stiffest and heaviest mesh implanted, was the most vulnerable to eliciting an immense foreign body response, irrespective of surgical technique. It is unclear exactly how long this negative remodelling process takes place and how complications like mesh exposures ensue. It is likely, however, that for most meshes negative remodelling proceeds to a point at which the forces equilibrate, and the remodelling response reaches homeostasis, as most women do not

experience mesh exposure. These observational findings of mesh-specific differences, although superficial, were in essence, indicators of the more robust remodeling occurring within the tissues, as subsequent smooth muscle outcomes measures also showed mesh-specific differences.

Gynemesh™ PS had the most significant impact on VaSM myofibre function and thickness. It is likely that the high stiffness mesh shielded the underlying soft tissues from experiencing normal physiological stress, thus inducing atrophy and thinning of the smooth muscle layer. This is particularly important, as women with POP show changes in smooth muscle function and peripheral nerve density relative to women without prolapse.<sup>14,25</sup> Additionally, the high weight and low porosity is likely to result in a greater mesh burden, and an increased likelihood of a heightened foreign body response, with impaired tissue ingrowth and a poor functional outcome. This is similar to cases where implantation of very stiff stents off-loaded the arterial wall, causing rapid and extensive atrophy of arterial smooth muscles.<sup>26–32</sup>

More interestingly, evidence of a significant impact on adrenergic nerve density, which was shown to be a function of mesh porosity, in both the grafted and non-grafted regions suggest that adrenergic nerves may be the most vulnerable to injury. It is also possible that its loss may precede, and possibly orchestrate, changes in the other smooth muscle components. The recent study by Northington et al. showed that women with POP exhibit a complete loss of response to the  $\alpha_1$ -adrenoreceptor agonist, phenylephrine, relative to non-prolapse controls.<sup>14</sup> Therefore, the perseverance of adrenergic nerve density following implantation with UltraPro™ perpendicular and Restorelle®, versus Gynemesh™ PS and UltraPro™ parallel, may explain the more favourable outcomes demonstrated. Alternatively, the observed decline in adrenergic nerve density following Gynemesh™ PS and UltraPro™ parallel implantation may explain the gross negative impact on VaSM. The results support the conclusion that high-stiffness meshes can have a negative effect on cholinergic nerves, as in the case of Gynemesh™ PS, but that lower stiffness meshes may have the potential to maintain or increase nerve density, a finding which is supported in the literature.<sup>33–38</sup>

## Conclusion

Overall, this study shows that mechanical and textile properties of the mesh can have a significant impact on smooth muscle outcomes. In particular, mesh stiffness and weight are negatively correlated with muscle outcomes, whereas porosity is positively correlated with muscle outcomes, supporting the transition to lightweight and large-pore meshes. Mesh stiffness also proved to have the most independent negative effect, especially on myofibre function, which was evident in both the underlying grafted tissues and in the tissues adjacent to the mesh. It is possible that the impact of one of the identified negatively correlated mesh properties, as observed with UltraPro™ parallel, could prove tolerable; however, a mesh exhibiting a combination of these, as shown in the case of Gynemesh™ PS, could lead to major complications. Future work will involve more studies to not only explore the mechanisms of mesh impact at later time points, but to also aid in designing new meshes to improve the postoperative degenerative effects following surgical mesh placement.

## Supplementary Material

Refer to Web version on PubMed Central for supplementary material.

## Acknowledgments

We would like to thank Leslie Meyn, MS, for her assistance with the statistical analysis, and Dr Yoshio Sugino, Ms Suzan Stein, and Ms Vickie Erickson for their technical expertise.

### Funding

Financial support was provided by the National Institutes of Health (NIH) R01 HD061811-01.

## References

- Olsen AL, Smith VJ, Bergstrom JO, Colling JC, Clark AL. Epidemiology of surgically managed pelvic organ prolapse and urinary incontinence. *Obstet Gynecol.* 1997; 89:501–6. [PubMed: 9083302]
- Subak LL, Waetjen LE, van den Eeden S, Thom DH, Vittinghoff E, Brown JS. Cost of pelvic organ prolapse surgery in the United States. *Obstet Gynecol.* 2001; 98:646–51. [PubMed: 11576582]
- Clark AL, Gregory T, Smith VJ, Edwards R. Epidemiologic evaluation of reoperation for surgically treated pelvic organ prolapse and urinary incontinence. *Am J Obstet Gynecol.* 2003; 189:1261–7. [PubMed: 14634551]
- Altman D, Vayrynen T, Engh ME, Axelsen S, Falconer C. Anterior colporrhaphy versus transvaginal mesh for pelvic-organ prolapse. *N Engl J Med.* 2011; 365:1826–1836.
- Maher CM. Surgical management of pelvic organ prolapse in women: the updated summary version Cochrane review. *Int Urogynecol J.* 2011; 22:1445–57. [PubMed: 21927941]
- Food and Drug Administration (FDA). Urogynecologic Surgical Mesh: Update on the Safety and Effectiveness of Transvaginal placement for pelvic Organ prolapse. FDA Administration E. 2001. [<http://www.fda.gov/medicalDevices/Safety/AlertsandNotices/ucm262435.htm>] Last Accessed 1 August 2013]
- Liang R, Abramowitch J, Knight K, Palcsey S, Nolfi A, Feola A, et al. Vaginal degeneration following implantation of synthetic mesh increased stiffness. *BJOG.* 2012; 120:233–43.
- Feola A, Abramowitch S, Jallah Z, Stein S, Barone W, Palcsey S, et al. Deterioration in biomechanical properties of the vagina following implantation of a high-stiffness prolapse mesh. *BJOG.* 2013; 120:224–32. [PubMed: 23240801]
- Shepherd J, Feola AJ, Stein S, Moalli P, Abramowitch SD, Moalli PA. Uniaxial biomechanical properties of 7 different vaginally implanted meshes for pelvic organ prolapse. *Int Urogyn J.* 2012; 23:613–20.
- Boreham MK, Wai CY, Miller RT, Schaffer JI, Word RA. Morphometric analysis of smooth muscle in the anterior vaginal wall of women with pelvic organ prolapse. *Am J Obstet Gynecol.* 2002; 187:56–63. [PubMed: 12114889]
- Ozdegirmenci O, Karslioglu Y, Dede S, Karadeniz S, Haberal A, Gunhan O, et al. Smooth muscle fraction of the round ligament in women with pelvic organ prolapse: a computer-based morphometric analysis. *Int Urogynecol J Pelvic Floor Dysfunct.* 2005; 16:39–43. discussion 43. [PubMed: 15365597]
- Takacs P, Gualtieri M, Nassiri M, Candiotti K, Fornoni A, Medina CA. Caldesmon expression is decreased in women with anterior vaginal wall prolapse: a pilot study. *Int Urogynecol J Pelvic Floor Dysfunct.* 2009; 20:985–90. [PubMed: 19582387]
- Inal HA, Kaplan PB, Usta U, Tastekin E, Aybatli A, Tokuc B. Neuromuscular morphometry of the vaginal wall in women with anterior vaginal wall prolapse. *Neurourol Urodyn.* 2010; 29:458–63. [PubMed: 19714736]

14. Northington GM, Basha M, Arya LA, Wein AJ, Chacko S. Contractile response of human anterior vaginal muscularis in women with and without pelvic organ prolapse. *Reprod Sci.* 2011; 18:296–303. [PubMed: 21193802]
15. Skoczylas LC, Jallah Z, Sugino Y, Stein SE, Feola A, Yoshimura N, et al. Regional differences in rat aging smooth muscle contractility and morphology. *J Reprod Sci.* 2013 Apr;20:382–90.
16. Yucel S, De Souza A Jr, Baskin LS. Neuroanatomy of the human female lower urogenital tract. *J Urol.* 2004; 172:191–5. [PubMed: 15201770]
17. Jia X, Glazener C, Mowatt G, MacLennan G, Bain C, Fraser C, et al. Efficacy and safety of using mesh or grafts in surgery for anterior and/or posterior vaginal wall prolapse: systematic review and meta-analysis. *Int J Obstet Gynecol.* 2008; 115:1350–61.
18. Maher C, Feiner B, Baessler K, Glazener CM. Surgical management of pelvic organ prolapse in women. *Cochrane Database Syst Rev.* 2010; 3(Issue 4):CD004014.
19. Wu JM, Kawasaki A, Hundley AF, Dieter AA, Myers ER, Sung VW. Predicting the number of women who will undergo incontinence and prolapse surgery, 2010 to 2050. *Am J Obstet Gynecol.* 2001; 205:230.e1–5.
20. Moshayedi P, Gilbert NG, Kwok JC, Yeo GS, Bryant CE, Fawcett JW, et al. The relationship between glial cell mechanosensitivity and foreign body reactions in the central nervous system. *J Biomaterials.* 2004; 39:3919–25.
21. Blakney AK, Swartzlander MD, Bryant SJ. The effects of substrate stiffness on the in vitro activation of macrophages and in vivo host response to poly(ethylene-glycol)-based hydrogels. *J Biomed Mater Res.* 2012; 100:1375–86.
22. Patel NR, Bole M, Chen C, Hardin CC, Kho AT, Mih J, et al. Cell elasticity determines macrophage function. *PLoS ONE.* 2012; 7:e41024. [PubMed: 23028423]
23. Fereol S, Fodil R, Galiacy S, Laurent VM, Louis B, Isabey D, et al. Sensitivity of alveolar macrophages to substrate mechanical and adhesive properties. *Cell Motil Cytoskeleton.* 2006; 63:321–40. [PubMed: 16634082]
24. Beningo KA, Wang YL. Fc-receptor-mediated phagocytosis is regulated by mechanical properties of the target. *J Cell Sci.* 2002; 115:849–56. [PubMed: 11865040]
25. Boreham MK, Miller RT, Schaffer JI, Word RA. Smooth muscle myosin heavy chain and caldesmon expression in the anterior vaginal wall of women with and without pelvic organ prolapse. *Am J Obstet Gynecol.* 2001; 185:944–52. [PubMed: 11641683]
26. Bayer IM, Adamson SL, Langille BL. Atrophic remodeling of the artery-cuffed artery. *Arterioscler Thromb Basc Biol.* 1999; 19:1499–505.
27. Heise RL, Parekh A, Joyce EM, Chancellor MB, Sacks MS. Strain history and TGF-beta1 induce urinary bladder wall smooth muscle remodeling and elastogenesis. *Biomech Model Mechanobiol.* 2012; 11:131–45. [PubMed: 21384200]
28. Jackson ZS, Dajnoweic D, Gotlieb A, Langille BL. Partial off-loading of longitudinal tension induces arterial tortuosity. *Arterioscler Thromb Basc Biol.* 2005; 25:957–62.
29. Deng L, Fairbank NJ, Cole DJ, Fredberg JJ, Maksym GN. Airway smooth muscle tone modulates mechanically induced cytoskeletal stiffening and remodeling. *J Appl Physiol.* 1985; 99:634–41.
30. Timmins LH, Miller MW, Clubb FJ, Moore JE. Increased artery wall stress post-stenting leads to greater intimal thickening. *Lab Invest.* 2011; 91:955–67. [PubMed: 21445059]
31. Gunst SJ, Tang DD, Opazo Saez A. Cytoskel remodeling of the airway smooth muscle cell: a mechanism for adaptation to mechanical forces in the lung. *Respir Physiol Neurobiol.* 2003; 137:151–68. [PubMed: 14516723]
32. Flavahan NA, Bailey SR, Flavahan WA, Mitra S, Flavahan S. Imaging remodeling of the actin cytoskeleton in vascular smooth muscle cells after mechanosensitive arteriolar constriction. *Am J Physiol Heart Circ Physiol.* 2005; 288:H660–9. [PubMed: 15388507]
33. Nomura H, Baladie B, Katayama Y, Morshead CM, Shoichet MS, Tator CH. Delayed implantation of intramedullary chitosan channels containing nerve grafts promotes extensive axonal regeneration after spinal cord injury. *Neurosurgery.* 2008a; 63:127–41. [PubMed: 18728578]
34. Man AJ, Davis HE, Itoh A, Leach JK, Bannerman P. Neurite outgrowth in fibrin gels is regulated by substrate. *Tissue Eng Part A.* 2011; 17:2931–41. [PubMed: 21882895]

35. Willerth SM, Sakiyama-Elbert SE. Approaches to neural tissue engineering using scaffolds for drug delivery. *Adv Drug Deliv Rev.* 2007; 59:325–38. [PubMed: 17482308]
36. Bakshi A, Fisher O, Daggi T, Himes BT, Fischer I, Lowman A. Mechanically engineered hydrogel scaffolds for axonal growth and angiogenesis after transplantation in spinal cord injury. *J Neurosurg Spine.* 2004; 1:322–9. [PubMed: 15478371]
37. Koch D, Rosoff WJ, Jiang J, Geller HM, Urbach JS. Strength in the periphery: growth cone biomechanics and substrate rigidity response in peripheral and central nervous system neurons. *Biophys J.* 2012; 102:452–60. [PubMed: 22325267]
38. Gu Y, Ji Y, Zhao Y, Liu Y, Ding F, Gu X, et al. The influence of substrate stiffness on the behavior and functions of schwann cell in culture. *Biomaterials.* 2012; 33:6672–81. [PubMed: 22738780]

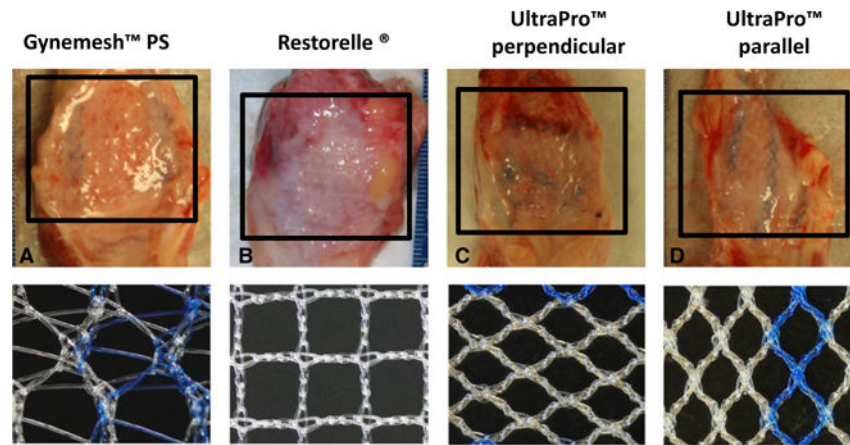


**Figure 1.**

Representative images of the anterior wall of the vagina at 3 months post-implantation (adapted from Feola et al.<sup>8</sup>) and their corresponding meshes (A–D). The half closest region to the cervix underlying the mesh was defined as the grafted region (boxed), and the lower portion adjacent to the mesh was defined as the non-grafted region. At the mesh–tissue interface of each mesh there was evidence of host tissue ingrowth, but the degree of incorporation varied depending on mesh-type. The less stiff meshes, UltraPro™ perpendicular and Restorelle®, had better incorporation of the tissue, whereas the stiffer Gynemesh™ PS appeared buckled and surrounded by a capsule of connective tissue (A).



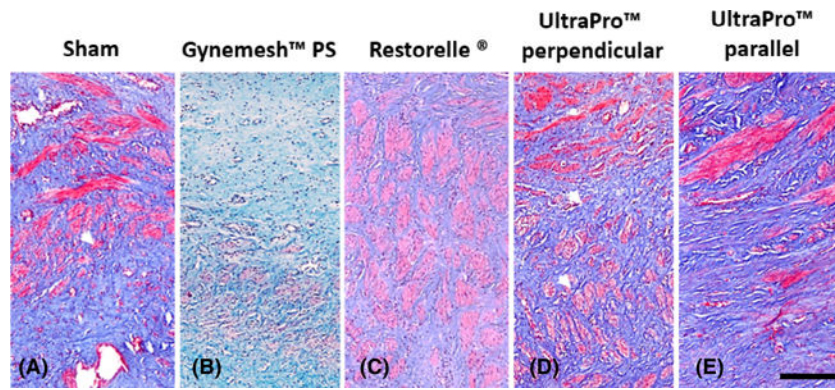


**Figure 2.** Representative images showing gross smooth muscle morphology following Masson's trichrome staining of grafted cross sections of (A) sham-operated, (B) Gynemesh™ PS, (C) Restorelle®, (D) UltraPro™ perpendicular, and (E) UltraPro™ parallel tissue biopsies. Compared with sham and UltraPro™ perpendicular, implantation with the higher stiffness meshes Gynemesh™ PS and UltraPro™ parallel were observed to have less smooth muscle bundles. Scale bar: 250  $\mu$ m.

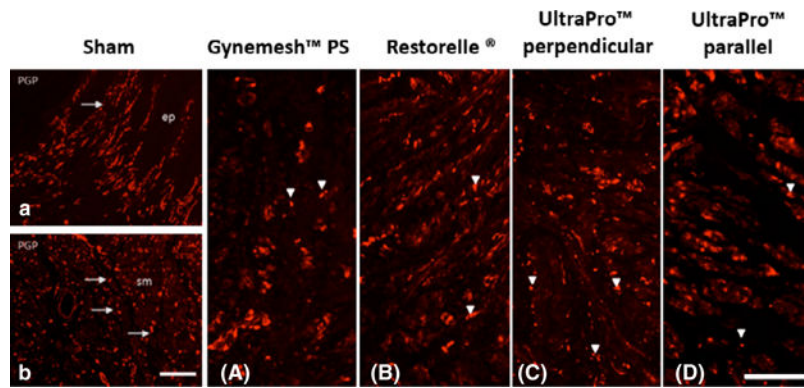


**Figure 3.**

Representative images of PGP 9.5 immunolabelling of grafted cross sections. The sham-operated group showed high levels of immunoreactivity (IR), indicative of the maintenance of peripheral nerve fibres, which were localised immediately below the epithelial layer (ep, top panel) and within muscularis (sm, lower panel). Following Gynemesh™ PS (A) and UltraPro™ parallel implantation, the nerve morphology of nerve fibres in the muscularis was altered, and nerve density was significantly reduced. Scale bars: 250  $\mu$ m.

**Table 1**

Macaque demographics

Variables	Mesh groups				P	
	Sham (n = 7)	Gynemesh™ PS (n = 7)	Restorelle® (n = 7)	UltraPro™ perpendicular (n = 6)		UltraPro™ parallel (n = 7)
Age (years)	15.0 (15.0–15.2)	13.5 (11.0–14.0)	13.0 (12.5–15.2)	13.0 (12.0–15.0)	13.0 (12.5–13.2)	P 0.132
Weight (g)	8.5 (8.0–9.3)	7.9 (7.1–9.0)	9.4 (8.3–12.5)	7.3 (6.4–8.8)	8.2 (8.0–9.2)	P 0.426
Parity	6.0 (3.5–6.5)	4.0 (2.0–5.2)	5.0 (3.0–5.2)	3.0 (2.2–6.5)	4.0 (4.0–5.5)	P 0.782

Values presented as medians (interquartile ranges). Significance set at  $P < 0.05$ .

**Table 2**

Muscle myofibre, nerve, and receptor function

	KCl (mN/mm <sup>2</sup> )		EFS (% KCl)		Carbachol (% KCl)	
	Grafted*	Non-grafted	Grafted	Non-grafted	Grafted	Non-grafted
Sham	0.24 (0.21–0.31)		39.6 (7.9–71.1)		7.9 (4.4–22.3)	79.1 (41.8–81.5)
Gynemesh™ PS	0.05 (0.01–0.07) *	0.19 (0.13–0.21)	9.4 (2.2–23.8) *	26.6 (16.6–37.7)	0.7 (0.0–9.5)	5.7 (2.7–17.4) *
Restorelle®	0.10 (0.10–0.18) *	0.18 (0.14–0.36)	43.4 (36.5–73.0)	22.3 (16.5–30.8)	61.2 (58.0–89.6) *	42.1 (37.5–76.1)
UltraPro™ perpendicular	0.17 (0.13–0.22)	0.40 (0.36–0.43)	49.9 (46.6–63.7)	25.7 (15.7–41.2)	30.4 (25.5–50.7)	39.7 (32.7–50.7)
UltraPro™ parallel	0.07 (0.04–0.12) *	0.17 (0.14–0.26)	32.2 (30.0–40.3)	30.5 (24.6–44.4)	31.8 (25.9–91.5)	65.8 (6.0–85.5)

Values above indicate maximum contraction following application of stimulant: median (interquartile range).

\* Carbachol response for sham is not presented as an average response because of significant differences between the proximal (grafted) and mid (non-grafted) response. Significance set at  $P < 0.05$ .

**Table 3**

Peripheral, cholinergic, and adrenergic nerve density

	Peripheral nerve density (% area)		Cholinergic nerve density (% area)		Adrenergic nerve density (% area)	
	Grafted	Non-grafted	Grafted	Non-grafted	Grafted	Non-grafted
Sham	0.53 (0.47–0.58)		0.020 (0.025–0.045)		0.20 (0.17–0.25)	
Gynemesh™ PS	0.05 (0.04–0.05)*	0.41 (0.13–0.42)	0.011 (0.010–0.020)	0.007 (0.005–0.012)*	0.01 (0.00–0.03)*	0.08 (0.07–0.11)*
Restorelle®	0.28 (0.19–0.30)	0.42 (0.33–0.50)	0.051 (0.042–0.054)	0.080 (0.047–0.091)	0.08 (0.06–0.09)	0.23 (0.18–0.30)
UltraPro™ perpendicular	0.25 (0.22–0.38)	0.30 (0.28–0.51)	0.052 (0.057–0.065)	0.096 (0.067–0.129)	0.14 (0.04, 0.17)	0.14 (0.13–0.14)
UltraPro™ parallel	0.16 (0.15–0.17)*	0.30 (0.20–0.41)	0.023 (0.005–0.048)	0.011 (0.016–0.022)	0.01 (0.00, 0.03)*	0.13 (0.09–0.13)*

Values represented as medians (interquartile ranges).

\* Indicates significance relative to sham ( $P < 0.05$ ).

**Table 4**

Regression analysis of mesh properties as predictors of smooth muscle outcomes

	Stiffness			Weight			Pore size		
	95% CI	P	95% CI	95% CI	P	95% CI	95% CI	P	P
<b>Grafted</b>									
KCl (myofiber function)	26.72 (11.61, 41.83)	<0.001*	0.35 (0.12, 0.59)	0.002*	-0.31 (-0.72, 0.08)	0.125			
EFS (nerve function)	6.79 (0.22, 13.35)	0.042*	0.15 (0.04, 0.07)	<0.001*	-0.14 (-0.27, -0.01)	0.033*			
Carbachol (receptor function)	-0.52 (-5.47, 4.41)	0.834	0.09 (0.06, 0.12)	<0.001*	-0.08 (-0.14, 0.03)	0.002*			
PGP 9.5 (nerve density)	15.62 (3.19, 28.06)	0.013*	0.26 (0.07, 0.46)	0.007*	-0.22 (-0.50, 0.06)	0.122			
VAcHT (cholinergic)	66.64 (14.43, 118.84)	0.012*	1.11 (0.69, 1.52)	<0.001*	-1.18 (-2.21, -0.14)	0.025*			
TH (adrenergic)	28.51 (-2.54, 59.57)	0.072	0.43 (-0.03, 0.91)	0.069	-0.27 (-0.91, 0.37)	0.404			
<b>Non-Grafted</b>									
KCl (myofiber function)	8.54 (7.86, 9.21)	<0.001*	0.35 (-5.70, 4.13)	0.754	0.01 (-0.10, 0.08)	0.847			
EFS (nerve function)	-1.63 (-4.26, 0.98)	0.222	-0.002 (-0.03, 0.03)	0.889	0.03 (-0.01, 0.07)	0.179			
Carbachol (receptor)	-0.35 (-4.42, 3.52)	0.856	0.05 (0.01, 0.08)	0.002*	-0.04 (-0.10, 0.01)	0.156			
PGP 9.5 (nerve density)	2.22 (0.00, 4.44)	0.049*	0.04 (0.03, 0.05)	<0.001*	-0.06 (-0.07, -0.04)	<0.001*			
VAcHT (cholinergic)	94.70 (-6.21, 195.61)	0.065	1.47 (-0.28, 3.24)	0.099	-1.18 (-2.21, -0.14)	0.025			
TH (adrenergic)	9.83 (-1.86, 21.54)	0.099	0.26 (0.19, 0.33)	<0.001*	-0.33 (-0.43, -0.23)	<0.001*			

KCl, potassium chloride; EFS, electrical field stimulation; PGP 9.5, protein gene product 9.5; TH, tyrosine hydroxylase; VAcHT, vesicular acetylcholine transporter.

Values above indicate maximum contraction following application of stimulant: estimate (upper confidence interval, lower confidence interval).

\* Significance set at  $P < 0.05$ .